Journal of Applied Physics ARTICLE scitation.org/journal/jap

Charge transport in an organic light emitting diode material measured using metal-insulator-semiconductor charge extraction by linearly increasing voltage with parameter variation

Cite as: J. Appl. Phys. **126**, 035501 (2019); doi: 10.1063/1.5100313
Submitted: 17 April 2019 · Accepted: 18 June 2019 ·
Published Online: 19 July 2019

Mile Gao,[1] Paul L. Burn,[1,a)] and Almantas Pivrikas[2,b)]

AFFILIATIONS

[1]Centre for Organic Photonics & Electronics (COPE), School of Chemistry and Molecular Biosciences, The University of Queensland, Brisbane, Queensland 4072, Australia
[2]School of Engineering and Information Technology, Murdoch University, Perth, Western Australia 6150, Australia

[a)]p.burn2@uq.edu.au
[b)]A.Pivrikas@murdoch.edu.au

ABSTRACT

Charge transport measurement using the Metal-Insulator-Semiconductor Charge Extraction by Linearly Increasing Voltage (MIS-CELIV) technique is a promising method for determining charge mobility in organic semiconductors because of its ability to study electron and hole mobilities independently. However, MIS-CELIV measurements have a number of parameters that can potentially affect the calculated mobility. There are only a few reports on MIS-CELIV being used to determine the charge mobility for materials typically used in organic light-emitting diodes (OLEDs), and the impact of each of the MIS-CELIV experimental parameters on the mobility is presently unknown. We find that the pulse duration, injection time, maximum voltage, offset voltage, and external load resistance have different levels of influence on the calculated mobility. Using the hole transporting OLED host material, tris(4-carbazoyl-9-ylphenyl)amine (TCTA), we show that having an injection time sufficient to fully charge the insulator layer, a pulse duration comparable to the transit time, and an external circuit time constant much smaller than the transit time is required to give a mobility relevant to an OLED. The optimized MIS-CELIV parameters led to the measurement having a similar current density and electric field to that of an operational OLED. Under these conditions, the hole mobility of TCTA was determined to be $2.90 \pm 0.07 \times 10^{-4}$ cm^2 V^{-1} s^{-1}, which is similar to that measured using time-of-flight techniques. Using inappropriate experimental parameters could lead to an underestimation of the mobility by an order of magnitude. Simulations of the MIS-CELIV measurements verified the effect the different parameters played in determining the charge mobility.

INTRODUCTION

The technological breakthrough by Tang and VanSlyke of the first thin film organic semiconductor electroluminescent device[1] catalyzed the development of commercial organic light-emitting diodes (OLEDs) for displays. OLEDs are particularly attractive as they can be flexible and ultrathin, have high efficiency and better light quality, and, in the context of OLED lighting, have a reduced hazard from deep blue/UV light.[2–5] OLEDs are often evaluated and compared based on their external quantum efficiency (EQE), which can be expressed as

$$\mathrm{EQE} = \phi_{capture} \times \phi_{spin} \times \phi_{PLQY} \times \phi_{escape} \times 100\%, \quad (1)$$

where $\phi_{capture}$ is the fraction of electrons and holes that recombine to form excitons, ϕ_{spin} is related to the spin statistics for the formation of singlet or triplet excitons, ϕ_{PLQY} is the photoluminescence quantum yield (PLQY) of the emissive layer, and ϕ_{escape} is the outcoupling efficiency. The EQE can be improved by optimizing each of the four parameters. For example, for isotropic emitters, ϕ_{escape} is around 20% due to the refractive indices of the materials used. However, by controlling the alignment of the emissive dipole

moment of the emitter or manipulating the refractive indices of the materials, it is possible to increase the outcoupling efficiency.[6,7] Furthermore, by careful design of the material, it is possible to have compounds that harvest both the singlet and triplet excitons, leading to ϕ_{spin} being 100%,[8–10] as well as them having a ϕ_{PLQY} of near unity.[11–13] $\phi_{capture}$ is the fraction of electrons and holes that combine to form excitons, which is strongly influenced by charge transport through the active layers in the device. Balanced charge injection and transport into and through the light-emitting layer is desired. To be able to design the optimized device architecture, it is necessary to have knowledge of the charge transporting capability of each of the materials in each of the layers within the OLED.

Popular methods to measure charge mobility in disordered materials include time-of-flight (ToF), space-charge-limited-current (SCLC), and organic field-effect transistors (OFETs). Standard ToF measurements require a very thick organic layer (>1 μm), which is much thicker than the practical thickness of the organic layers used in OLEDs (normally <100 nm), which is an issue as mobility can have a thickness dependence.[14] SCLC measurements require blocking electrodes to create "hole-only" and "electron-only" devices. Implementation of such electrodes is not always easy in practice and if the devices are leaky or if the materials have intrinsic doping or charge traps, then the analysis can be unreliable or complex. The mobilities from OFET measurements are not comparable to those from diode architectures as the current is confined to a thin layer at the interface with the dielectric layer, giving rise to mobilities at least an order of magnitude larger than mobilities measured by ToF.[15]

In order to overcome these limitations, a method employing charge extraction by linearly increasing voltage based on a metal-insulator-semiconductor structure diode architecture (MIS-CELIV) has been developed and used for measuring the charge mobility in organic bulk heterojunction solar cells.[16] First, by applying a sufficiently large injecting (offset) bias, it is possible to inject a single charge carrier type through the semiconductor, either holes or electrons, to the semiconductor/insulator interface. Then, a linearly increasing voltage extracts those injected charges back to the electrode. The time it takes for the transient to reach the maximum during extraction is defined as the transit time (t_{max}), and following the method developed by Juška *et al.*,[17] it is possible to calculate the mobility from the following equation:

$$\mu = \frac{2d_s^2}{At_{max}^2}\left(1+\frac{\varepsilon_s d_i}{\varepsilon_i d_s}\right), \tag{2}$$

where d_s is the thickness of the semiconducting layer; d_i is the thickness of the insulating layer; A is the extraction speed, which is the slope of rising voltage U, $\mathrm{d}U/\mathrm{d}t$; ε_s is the relative permittivity of the organic semiconductor; and ε_i is the relative permittivity of an insulator. Advantages of MIS-CELIV are that it can be used to selectively measure either hole or electron mobilities in films with thicknesses close to those used in operational devices. MIS-CELIV has been used for the determination of the charge mobility in the active layer of bulk heterojunction solar cells. In terms of OLEDs, there have only been two reports where the technique has been used for the study of mobility. In both cases, MIS-CELIV measurements were undertaken to determine the hole mobility in a standard hole transporting material, namely, *N*,*N*′-bis(1-naphthyl)-*N*,*N*′-diphenyl-1,10-biphenyl-4,4′-diamine.[18,19] However, in the reported measurements, only the effect of different offset voltages was studied,[18,19] with the work ignoring the other critical parameters including the extraction voltage, pulse duration (also known as extraction time), external load resistance, and so on, which are all critical in understanding the measured mobilities. These parameters can in principle change the shape of transients and hence need to be accounted for in mobility calculations based on the MIS-CELIV measurements.

Therefore, in this paper, we explore the effect of the MIS-CELIV parameters on the measured mobilities in an organic semiconductor thin film. In particular, we vary pulse duration, offset voltage, maximum pulse voltage, injection time (at offset voltage), and the external load resistance. We undertake a series of MIS-CELIV measurements on evaporated films of tris (4-carbazoyl-9-ylphenyl)amine (TCTA), which is commonly used in OLEDs as a hole transporting or host material. TCTA has been reported to have a good hole mobility and a large optical gap.[20–22] The chemical structure of TCTA and a schematic of the

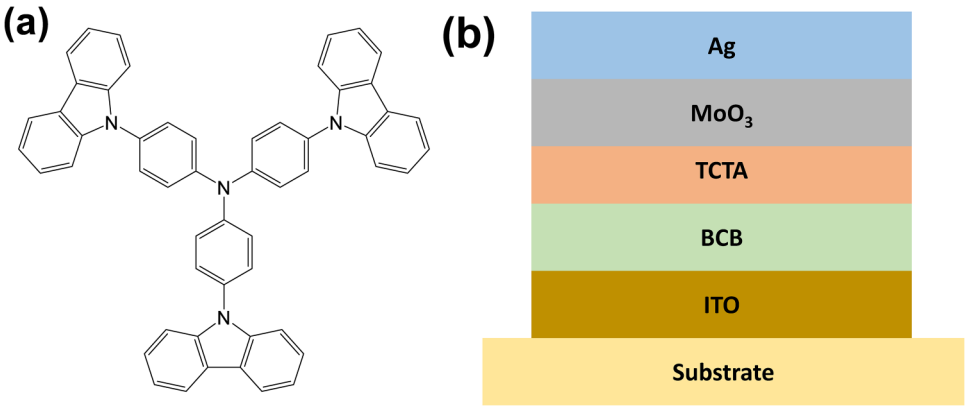

FIG. 1. Chemical structure of TCTA (a) and schematic device structure (b). Ag = silver, MoO_3 = molybdenum oxide, BCB = thermally annealed Cyclotene 3022-35, ITO = indium tin oxide, and substrate = glass.

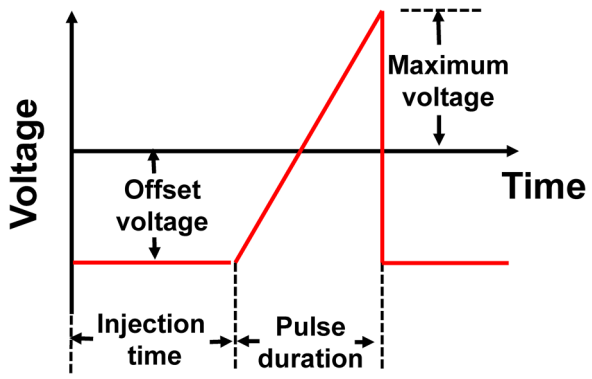

FIG. 2. Illustration of a model MIS-CELIV experiment defining each of the parameters in an applied pulse.

MIS-CELIV device architecture are depicted in Fig. 1. Finally, we report numerical simulations of the MIS-CELIV transients to predict the functional dependence of charge mobility values on the experimental parameters.

RESULTS AND DISCUSSION

The parameters for a typical MIS-CELIV measurement are shown in Fig. 2. The offset voltage is defined as the bias applied to achieve charge injection, which in the current work is hole injection through the semiconductor to the interface with the BCB insulator. The time over which the offset voltage is applied is defined as the injection time. The pulse duration or extraction time is the time during which the linearly increasing voltage is applied until the maximum voltage is reached, with the voltage increase starting at 0 s. An external load resistance, forming a series circuit with the sample acting as a capacitor, is connected to an oscilloscope input in parallel to adjust the magnitude of the transient signals. Unless further specified, all the measurements were carried out with a 50 Ω external resistance and a 500 ms injection time.

In the first part of the study to determine the effect of each of the parameters on the measured mobility, we set the offset and maximum voltages at −10 V and 10 V, respectively, while changing the pulse duration. Figures 3(a) and 3(b) show the applied pulses and measured results with different pulse duration. The hole mobilities were calculated according to Eq. (2) and were also simulated [Fig. 3(c)]. The hole mobility of TCTA measured with a 5 μs pulse duration was $2.90 \pm 0.07 \times 10^{-4}$ cm^2 V^{-1} s^{-1},

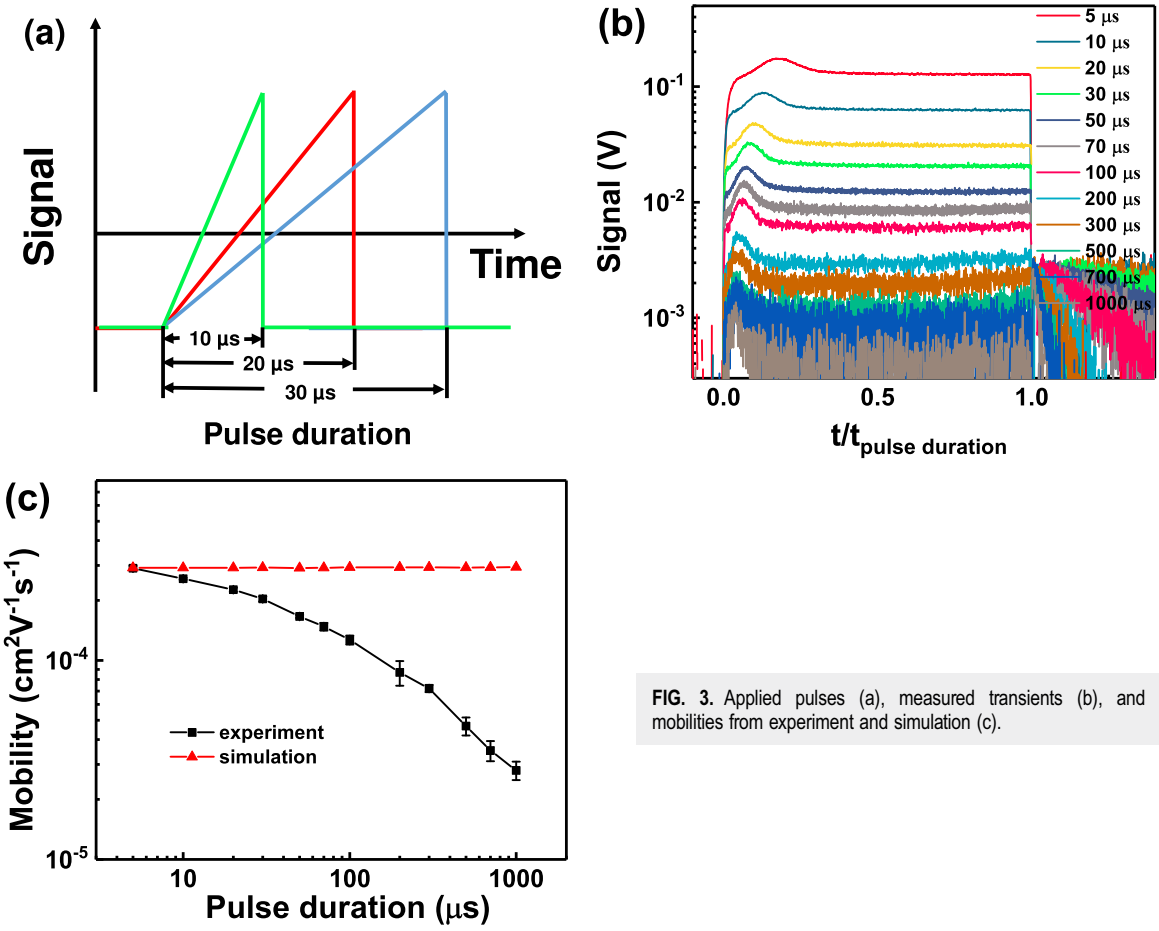

FIG. 3. Applied pulses (a), measured transients (b), and mobilities from experiment and simulation (c).

which was comparable with previous reports using ToF ($2–3 \times 10^{-4}$ cm^2 V^{-1} s^{-1}).[23,24] The error in the mobility arises from sample-to-sample variation. It was found that when the pulse duration was increased, the mobility values calculated using Eq. (2) decreased, reaching a low of $2.80 \pm 0.30 \times 10^{-5}$ cm^2/V^{-1} s^{-1} when a 1 ms pulse duration was used.

In order to check whether the observed decrease in the mobility is caused by a time dependent mobility or by the MIS-CELIV technique, we have performed numerical simulations. The trend of the experimental mobilities with pulse duration was different from that obtained by the simulations. Comsol Multiphysics software was used for the simulations to predict the experimentally measured mobility values. The numerical simulations represent a one-dimensional and nondispersive charge transport model with two materials of different dielectric permittivities (for the insulator and the semiconductor), and the boundary and initial conditions used have been reported before.[25] The simulations were performed using normalized parameter units to speed up the calculations and reduce errors. The normalized units of the parameters were then converted to specific measured values to fit the experimental data.

It can be seen in Fig. 3(c) that the mobility measured with the shortest pulse duration is closest to the simulated nondispersive (time-independent) charge transport mobility. When the pulse duration was increased, the deviation from the calculated mobility increases. This difference is caused by the delayed extraction of charges as the applied triangle voltage increases. As it will be seen from the next experiment, the injection of charges does not take place until a certain applied voltage. A complex distribution of the electric field inside the semiconductor can arise from interfacial effects and cause the perturbation of the voltage at which the charge extraction starts. Dispersive transport contributes to this effect as it makes the time to reach t_{max} longer and charge transport slower when longer duration pulses are applied.[26] However, note that the extraction transient reaches the displacement current plateau after the charge extraction is finished, meaning that the amount of trapped charge is minimal. Voltages used in the MIS-CELIV experiments lie within the normal OLED operating voltages (≈3–10 V) and given that the film thicknesses in both types of devices are not dissimilar, the two types of devices will have similar electric fields across the organic semiconductor layer (3.5×10^7 V/m for MIS-CELIV vs $\approx 3 \times 10^7$ V/m to $\approx 1 \times 10^8$ V/m

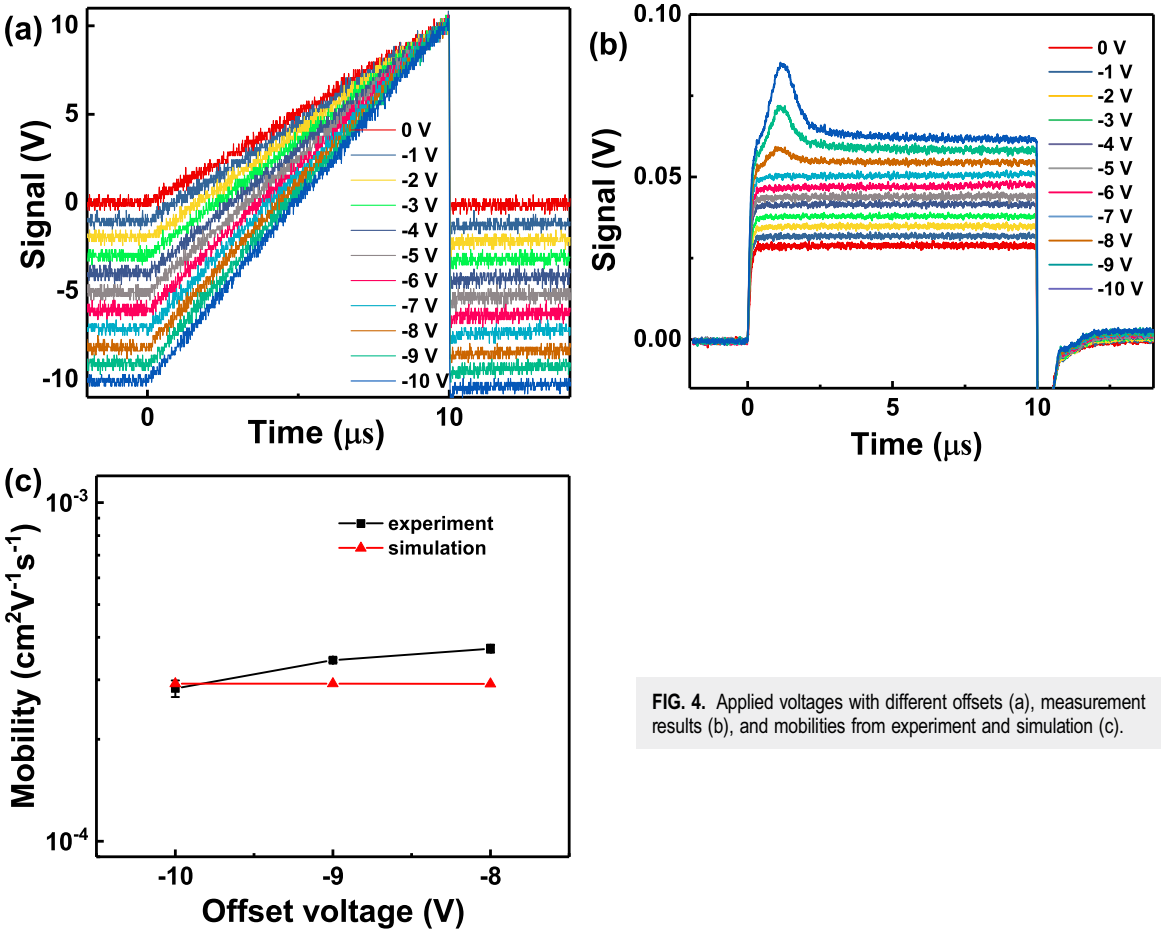

FIG. 4. Applied voltages with different offsets (a), measurement results (b), and mobilities from experiment and simulation (c).

for a typical operational OLED). Therefore, the mobility measured with a 5 μs pulse should be similar to the mobility of a neat film of TCTA in a working OLED.

We next varied the offset voltage while keeping the other parameters constant. As shown in Fig. 4(a), the offset voltage was increased to more negative biases, from 0 to −10 V. The pulse duration was kept constant at 10 μs, and the maximum voltage was kept at 10 V. Figure 4(b) shows the measured transients. When the offset voltage was more positive than −8 V, no peak was observed in the transients, indicating that there were no charge injection and the contact was blocking. When the offset voltage reached −8 V, the electric field was large enough to inject holes that could accumulate at the interface of the insulating and TCTA semiconducting layers. With a linearly increasing voltage, the injected charges were extracted with a peak observed in the current transient. Figure 4(c) shows the mobilities obtained by experiment and compared with simulation. At more negative offset voltages, the measured mobility was similar to the one predicted from the simulations. It is important to note that the current density at t_{max} for a −10 V offset voltage is 38 mA/cm^2, which is within the same range of the current density in an operating OLED,[27,28] again illustrating the relevance of the MIS-CELIV measurements to a working OLED. We found that less negative offset voltages that still allowed charge injection gave rise to a slightly higher measured mobility. However, the key point is that the magnitude of the offset voltage does not have a dramatic effect on the measured mobilities as long as the semiconductor/insulator has had sufficient amount of time to charge.

In the third part of the study, we varied the maximum voltages applied during the pulse for extracting the charges while keeping the pulse duration (10 μs) and offset voltage (−10 V) the same. We used an offset voltage of −10 V as it gave mobilities closest to the simulation. The same offset voltage and injection time meant that there were the same number of injected charges in all cases. The applied pulse voltages are shown in Fig. 5(a), and the corresponding transients are shown in Fig. 5(b). In the MIS-CELIV experiment, the applied electric field is not constant, changing linearly. To give a rough estimate of the average voltage in our experiment, we take the voltage at the time when the charge extraction current is largest (t_{max}). The experimentally estimated mobility is plotted as a function of this average voltage in Fig. 5(c). The simulation model has no field dependence, while the experimental mobility does follow a typical weak Poole-Frenkel-type

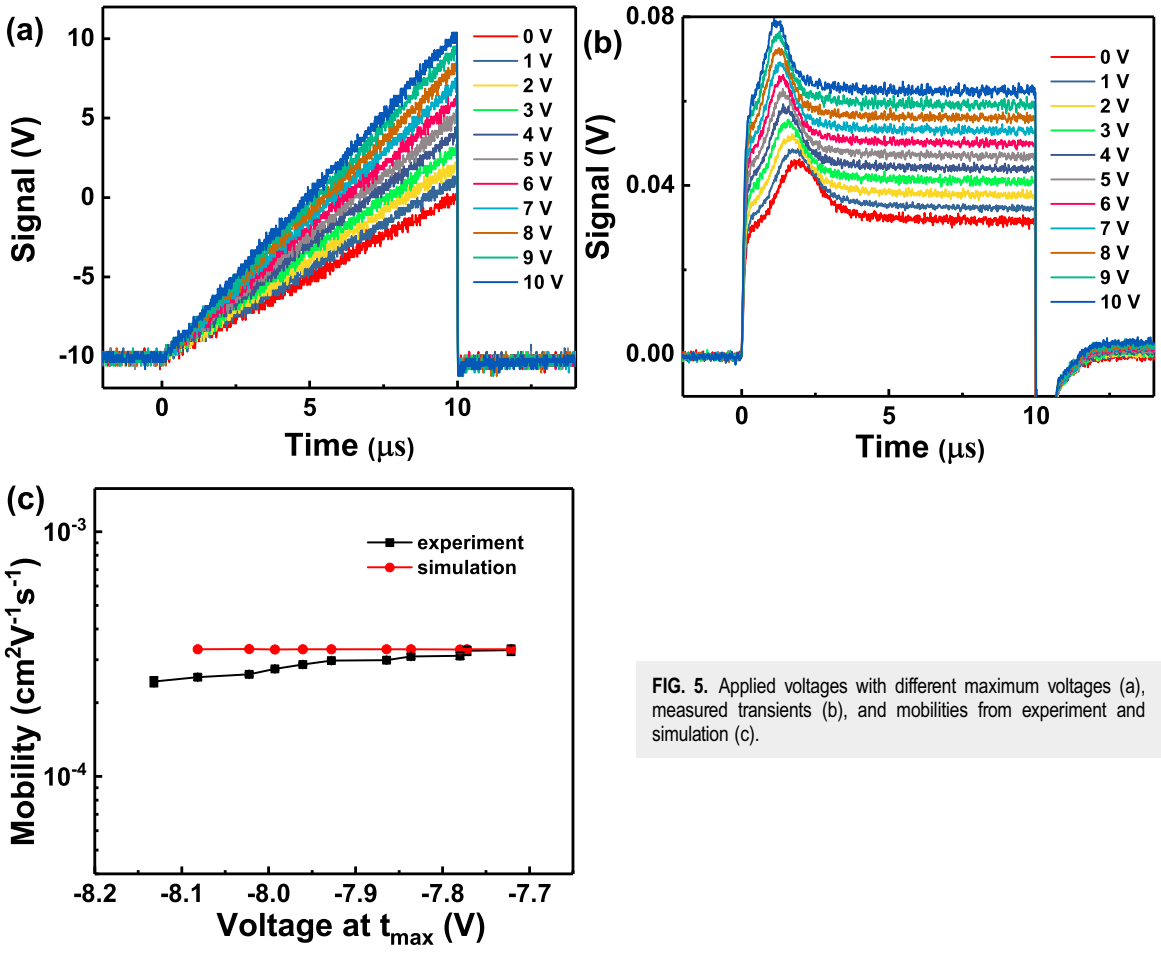

FIG. 5. Applied voltages with different maximum voltages (a), measured transients (b), and mobilities from experiment and simulation (c).

dependence on the electric field.[29,30] However, it is important to note that the applied electric field changes, hence in this experiment, the functional slope estimation of mobility dependence on the electric field is unreliable.

The fourth parameter that we considered was the time that the device was held at the offset voltage (−10 V), which is defined as the injection time [Fig. 6(a)]. For the measurements, the maximum voltage was 10 V and the pulse duration was 10 μs. During the injection time, charges are injected through the organic layer and accumulate at the interface with the insulating layer. We used the following injection times: 10 μs, 40 μs, 90 μs, 190 μs, 490 μs, 990 μs, 500 ms, and 1 s (note the 500 ms and 1 s injection times include the pulse duration, which was 10 μs), and the results are shown in Fig. 6(b). When the injection time was longer than 990 μs, the transients were almost identical, indicating that the number of injected charges had saturated. In other words, the insulator capacitor was fully charged. However, when the injection time became more comparable with the pulse duration, the signal was found to decrease and the transient peak shifted to a longer extraction time. We found that an injection time of 10 μs was too short for the number of injected charges to saturate, resulting in an almost flat transient. The number of injected charges was calculated by integrating the extraction current over time (the area under the transient peaks), plotted in Fig. 6(c). The injected charges increased from less than 2×10^{-10} C with a 10 μs injection time, saturating to 6.4×10^{-10} C for 990 μs and longer injection times. The extraction peak was also found to depend on the amount of injected charge, as seen from Fig. 6(b). Previous experiments showed that there was minimal charge trapping in the TCTA films, and the fact that all the charge can be extracted confirms the absence of deep traps, which is a critical requirement for efficient OLED devices. The calculated mobility based on the experimental data is also shown in Fig. 6(c). The apparent mobility increased along with a longer injection time before reaching a steady state. The results show that if the injection time is too short the measured mobility can be underestimated by up to an order of magnitude, and hence, sufficiently long injection times, which allow the insulator to be fully charged, are important.

Lastly, we measured the impact of the external circuit resistance on the extraction times. With a larger external resistance, the voltages measured on the oscilloscope for the current transient are larger, which facilities the observation of t_{max}. However, an increased external resistance gives rise to a larger RC time constant.

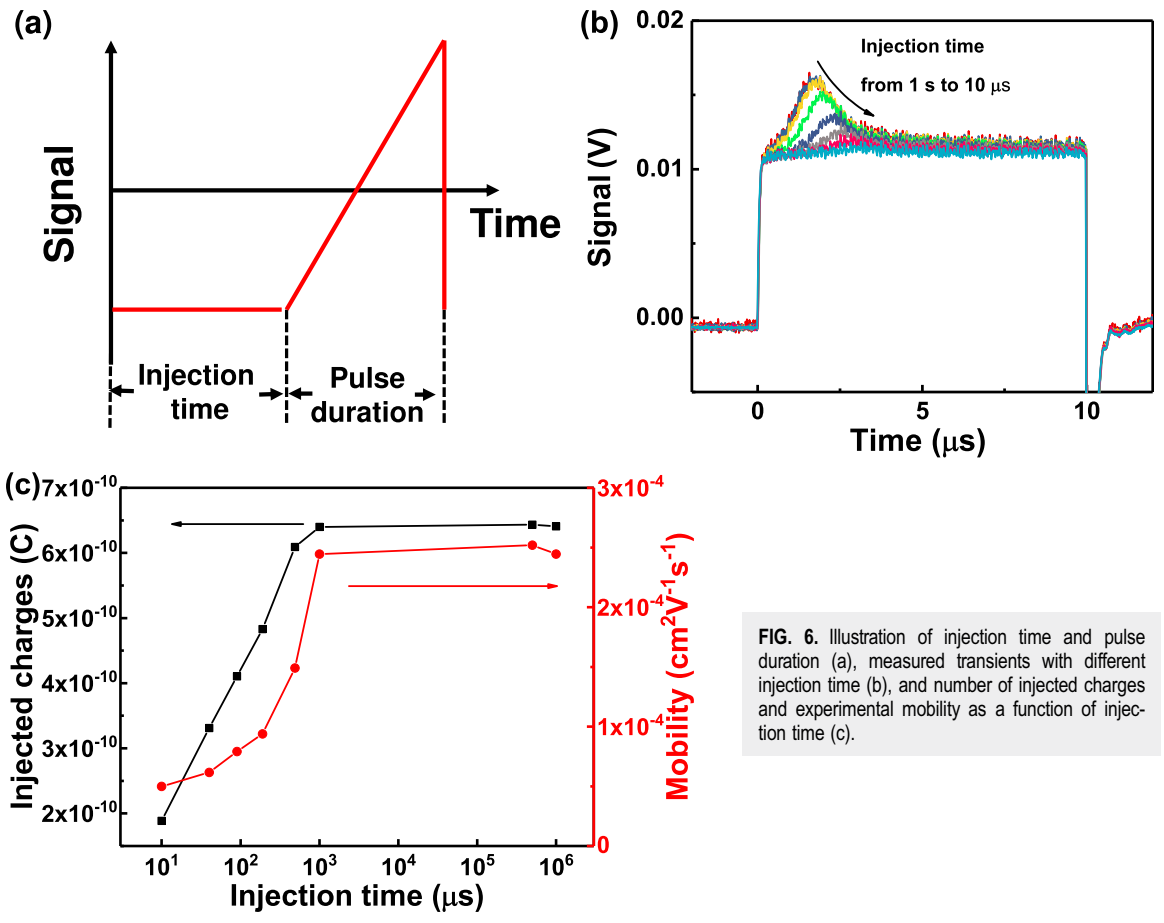

FIG. 6. Illustration of injection time and pulse duration (a), measured transients with different injection time (b), and number of injected charges and experimental mobility as a function of injection time (c).

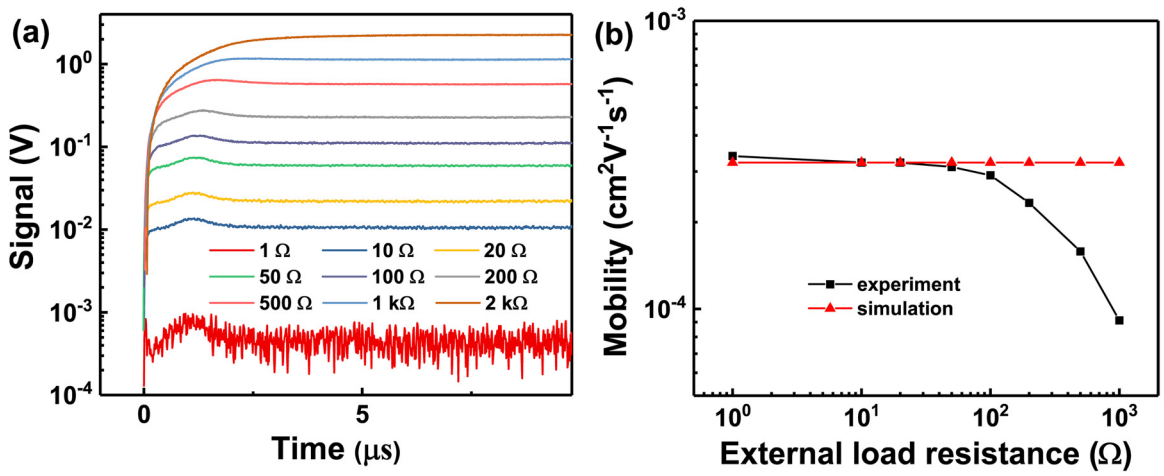

FIG. 7. MIS-CELIV measurement results with different external load resistances (a) and corresponding mobilities calculated from experiment and simulation (b).

The RC time constant was calculated using

$$RC = R(\varepsilon_0 \varepsilon_s S/d_i), \quad (3)$$

where $\varepsilon_0 = 8.85 \times 10^{-12}$ F/m, $\varepsilon_s = 3$, S (active area) $= 4.46 \times 10^{-6}$ m^2, $d_i = 50$ nm, and R ranges from 1 Ω to 2 kΩ. Thus, in these experiments, the RC time constant ranges from 0.002 μs to 4.8 μs. Figure 7 shows the measurement results when using different external load resistances. When the resistance was increased, the RC effect became pronounced. The extraction time became longer, eventually leading to a decrease in the calculated hole mobility. Figure 7(b) clearly shows the deviation of the experimentally measured mobility with higher resistances. Matching mobility values between simulation and experiment were observed when the RC was low and in particular when it is much lower than the extraction or transit time. Hence, in the MIS-CELIV experiment, the RC should be minimized to enable the reliable determination of t_{max} and hence the mobility.

CONCLUSION

In conclusion, this work applies MIS-CELIV to determine the hole mobility in evaporated thin films of TCTA and demonstrates how the different measurement parameters can affect the mobility calculation. The MIS-CELIV parameters that had a large effect on the measured mobility were triangle pulse duration, injection time, and the RC. Simulations were carried out to verify and predict the impact of each parameter. The decrease of measured mobility with increasing pulse duration shows that the correct mobility values should be determined from the shortest possible pulse duration. The injection time should be large enough to ensure saturation of the injected charges and their accumulation at the semiconductor/insulator interface. A shorter injection time results in the underestimation of the mobility. Finally, the external resistance should be minimized, because when RC is much larger than transit time, RC charging leads to an artificially extended t_{max} and thus a mobility lower than the true value. Considering all of these conditions, the hole mobility of TCTA using MIS-CELIV was determined to be $2.90 \pm 0.07 \times 10^{-4}$ cm^2 V^{-1} s^{-1}. The measurements also show that films comprised of neat evaporated TCTA are essentially trap free with respect to hole transport.

EXPERIMENTAL

4-in. Borofloat 33 glass wafers with a thickness of 0.5 mm were cleaned in an ultrasonic bath with acetone and then with *iso*-propanol. A 100 nm thick indium tin oxide (ITO) layer was sputter-coated onto the cleaned wafers using an AJA ATC-2200 sputtering system. AZ 6615 photoresist was spin-coated onto the ITO layer at 4000 rpm and then baked at 110 °C for 1 min. After baking, the films were exposed to UV light through a chrome photomask to define the pattern. The wafers were then dipped in the AZ 726 MIF developer to remove exposed photoresist area, and then 8M hydrochloric acid was used to etch the ITO pattern. Finally, the wafers were diced and the ITO substrates were dipped in acetone to remove remaining photoresist and then cleaned sequentially using de-ionized water with Alconox detergent, de-ionized water, acetone, and *iso*-propanol in an ultrasonic bath. The cleaned chips were blown dry with nitrogen and put in UV-ozone cleaner for 30 min to improve the work function as well as cleanliness. Cyclotene 3022-35 (BCB, Dow Chemical Company) was spin-coated in a nitrogen-filled glovebox onto the cleaned ITO chips at 5000 rpm to form a 50 nm thick layer that was then baked at 300 °C for 10 min. Then, samples with the annealed BCB layer were transferred into an evaporation chamber. Deposition of the TCTA started when the pressure decreased to less than 5×10^{-7} Torr and ended when the film thickness reached 180 nm. In the MIS-CELIV experiments, we made the semiconductor film a few times thicker than the insulator layer. We used a 50 nm thick insulator BCB layer to avoid pinholes and a 180 nm thick semiconductor layer. Finally, an 8 nm thick MoO_3 layer and a 90 nm thick Ag layer were sequentially deposited. The MIS-CELIV measurements were carried out using

a Waverunner 6200A oscilloscope (from LeCroy Corporation) and an Agilent 33250A function generator (from Agilent Technologies Inc.). The thickness of the BCB layer was measured using a DektakXT.

ACKNOWLEDGMENTS

The work was carried at the Centre for Organic Photonics & Electronics at The University of Queensland. P.B. is an Australian Research Council Laureate Fellow (No. FL160100067), and the work was supported by the Fellowship. We acknowledge financial support from the program of the China Scholarship Council (CSC, No.201707090077) for M.G. This work was performed in part at the Queensland node of the Australian National Fabrication Facility (ANFF-Q), a company established under the National Collaborative Research Infrastructure Strategy to provide nano- and microfabrication facilities for Australia's researchers.

REFERENCES

[1]C. W. Tang and S. A. VanSlyke, Appl. Phys. Lett. **51**, 913 (1987).
[2]A. Salehi, S. Ho, Y. Chen, C. Peng, H. Yersin, and F. So, Adv. Opt. Mater. **5**, 1700197 (2017).
[3]D.-H. Cho, O. E. Kwon, Y.-S. Park, B. G. Yu, J. Lee, J. Moon, H. Cho, H. Lee, and N. S. Cho, Org. Electron. **50**, 170 (2017).
[4]M. Singh, J.-H. Jou, S. Sahoo, S. Sujith, Z.-K. He, G. Krucaite, S. Grigalevicius, and C.-W. Wang, Sci. Rep. **8**, 7133 (2018).
[5]G. Li, T. Fleetham, E. Turner, X. C. Hang, and J. Li, Adv. Opt. Mater. **3**, 390 (2015).
[6]J. Frischeisen, D. Yokoyama, A. Endo, C. Adachi, and W. Brütting, Org. Electron. **12**, 809 (2011).
[7]H. Shin, J. H. Lee, C. K. Moon, J. S. Huh, B. Sim, and J. J. Kim, Adv. Mater. **28**, 4920 (2016).
[8]S. C. Lo, R. N. Bera, R. E. Harding, P. L. Burn, and I. D. W. Samuel, Adv. Funct. Mater. **18**, 3080 (2008).
[9]C. A. Strassert, C. H. Chien, M. D. Galvez Lopez, D. Kourkoulos, D. Hertel, K. Meerholz, and L. De Cola, Angew. Chem. Int. Ed. **50**, 946 (2011).
[10]Y. Ma, C. M. Che, H. Y. Chao, X. Zhou, W. H. Chan, and J. Shen, Adv. Mater. **11**, 852 (1999).
[11]S. Y. Kim, W. I. Jeong, C. Mayr, Y. S. Park, K. H. Kim, J. H. Lee, C. K. Moon, W. Brütting, and J. J. Kim, Adv. Funct. Mater. **23**, 3896 (2013).
[12]K.-H. Kim, S. Lee, C.-K. Moon, S.-Y. Kim, Y.-S. Park, J.-H. Lee, J. W. Lee, J. Huh, Y. You, and J.-J. Kim, Nat. Commun. **5**, 4769 (2014).
[13]S. Gambino, S. G. Stevenson, K. A. Knights, P. L. Burn, and I. D. Samuel, Adv. Funct. Mater. **19**, 317 (2009).
[14]M. Khan, W. Xu, Khizar-ul-Haq, Y. Bai, X. Jiang, Z. Zhang, W. Zhu, Z. Zhang, and W. Zhu, J. Appl. Phys. **103**, 014509 (2008).
[15]C. Tanase, E. Meijer, P. Blom, and D. De Leeuw, Phys. Rev. Lett. **91**, 216601 (2003).
[16]A. Armin, G. Juska, M. Ullah, M. Velusamy, P. L. Burn, P. Meredith, and A. Pivrikas, Adv. Energy Mater. **4**, 1300954 (2014).
[17]G. Juška, N. Nekrašas, and K. Genevičius, J. Non-Cryst. Solids **358**, 748 (2012).
[18]S. Züfle, S. Altazin, A. Hofmann, L. Jäger, M. T. Neukom, T. D. Schmidt, W. Brütting, and B. Ruhstaller, J. Appl. Phys. **121**, 175501 (2017).
[19]C. Katagiri, T. Yoshida, M. S. White, C. Yumusak, N. S. Sariciftci, and K.-I. Nakayama, AIP Adv. **8**, 105001 (2018).
[20]Y. Kuwabara, H. Ogawa, H. Inada, N. Noma, and Y. Shirota, Adv. Mater. **6**, 677 (1994).
[21]D. Dong, J. Xia, S. Yang, X. Wu, B. Wei, L. Lian, D. Feng, Y. Zheng, and G. He, Org. Electron. **38**, 29 (2016).
[22]B. S. Kim and J. Y. Lee, Adv. Funct. Mater. **24**, 3970 (2014).
[23]W.-Y. Hung, P.-Y. Chiang, S.-W. Lin, W.-C. Tang, Y.-T. Chen, S.-H. Liu, P.-T. Chou, Y.-T. Hung, and K.-T. Wong, ACS Appl. Mater. Interfaces **8**, 4811 (2016).
[24]S. Noh, C. Suman, Y. Hong, and C. Lee, J. Appl. Phys. **105**, 033709 (2009).
[25]B. Philippa, R. White, and A. Pivrikas, Appl. Phys. Lett. **109**, 153301 (2016).
[26]A. J. Mozer, G. Dennler, N. Sariciftci, M. Westerling, A. Pivrikas, R. Österbacka, and G. Juška, Phys. Rev. B **72**, 035217 (2005).
[27]J. Song, K.-H. Kim, E. Kim, C.-K. Moon, Y.-H. Kim, J.-J. Kim, and S. Yoo, Nat. Commun. **9**, 3207 (2018).
[28]J.-J. Huang, Y.-H. Hung, P.-L. Ting, Y.-N. Tsai, H.-J. Gao, T.-L. Chiu, J.-H. Lee, C.-L. Chen, P.-T. Chou, and M.-K. Leung, Org. Lett. **18**, 672 (2016).
[29]J. Frenkel, Phys. Rev. **54**, 647 (1938).
[30]M. Stolterfoht, S. Shoaee, A. Armin, H. Jin, I. Kassal, W. Jiang, P. Burn, and P. Meredith, Adv. Energy Mater. **7**, 1601379 (2017).